International Journal of Automotive Technology, Vol. 6, No. 6, pp. 665–670 (2005)

1229–9138/2005/024–14

POLYPROPYLENE/CLAY NANOCOMPOSITES FOR AUTOMOTIVE APPLICATIONS

C. H. HONG[1)], Y. B. LEE[1)], J. Y. JHO[1)], B. U. NAM[2)*] and T. W. HWANG[3)]

[1)]Hyperstructured Organic Materials Research Center and School of Chemical Engineering, Seoul National University, Seoul 151-742, Korea
[2)]Department of Applied Chemical Engineering, Korea University of Technology and Education, Chungnam 330-708, Korea
[3)]Polymeric Materials Research Team, Research & Development Division for Hyundai Motor Company & Kia Motor Company, 772-1 Changduk-dong, Whasung-si, Gyeonggi 445-706, Korea

(Received 13 August 2004; Revised 31 October 2005)

ABSTRACT–Nanocomposites of polypropylene with organically modified clays were compounded on a twin-screw extruder by two-step melt compounding of three components, i.e., polypropylene, maleic anhydride grafted polypropylene (PP-*g*-MA), and organically modified clay. The effect of PP-*g*-MA compatibilizers, including PH-200, Epolene-43, Polybond-3002, Polybond-3200, with a wide range of maleic anhydride (MA) content and molecular weight was examined. Morphologies of nanocomposites and their mechanical properties such as stiffness, strength, and impact resistance were investigated. X-ray diffraction patterns showed that the dispersion morphology of clay particles seemed to be determined in the first compounding step and the further dispersion of clays didn't occur in the second compounding step. As the ratio of PP-*g*-MA to clay increased, the clay particles were dispersed more uniformly in the matrix resin. As the dispersibility of clays was enhanced, the reinforcement effect of the clays increased, however impact resistance decreased.

KEY WORDS : Polypropylene, Nanocomposite, Clay, Stiffness, Impact resistance

1. INTRODUCTION

Recently polypropylene (PP) is considered as one of the promising materials to replace engineering plastics. In order to improve polypropylene's competitiveness in engineering resin application, it is necessary to simultaneously increase dimensional stability, heat distortion temperature, stiffness, and impact resistance without sacrificing easy processability. The production of polypropylene composites containing fiber reinforcement requires special processing technology involving fiber impregnation and prepreg formation (Im *et al.*, 2003). Therefore extensive studies are being placed upon the development of filled polypropylene, which is produced by means of conventional melt processing technology. Traditional fillers for polypropylene are calcium carbonate, talc, glass fiber, wollastonite, mica, glass beads, and wood flour. Filled PP containing talc is used extensively because of a combination of stiffness, dimensional stability, and importantly low cost. It is well known that filler anisotropy is especially favorable in matrix reinforcement. Although anisotropic nanofillers were expected to afford attractive combinations of stiffness and toughness, limited commercial availability and dispersion problems due to strong interparticle interactions of nanofillers have limited their application. One of the most common nanoscopic fillers is derived from montmorillonite (MMT) clay, which is found naturally in a layered silicate structure with a high surface area, about 750 m^2/g. The clay exists in a tactoid structure of 20–25 layers. Exchanging the cations in between the silicate layers with the bulkier and more organophilic cations alters the clay structure known as organoclay. This expansion of the clay layer or basal spacing makes it possible to be intercalated and exfoliated.

Nanocomposites based on organic polymers and inorganic clay materials consisting of silicate layers have attracted a great interest, because they have shown dramatic improvements in mechanical, thermal, and barrier properties with a small amount of layered silicates. A large number of polymer/clay nanocomposites have been studied including polystyrene (Vaia *et al.*, 1996), polyamide (Wu *et al.*, 2002; Fornes *et al.*, 2001), polyimide (Tyan *et al.*, 1999), epoxy resin (Frohlich *et al.*, 2003),

*Corresponding author. e-mail: bunam@kut.ac.kr

polypyrrole (Kim *et al.*, 2002), poly(ethylene oxide) (Lim *et al.*, 2003), poly(butyleneterephthalate) (Li *et al.*, 2001), and polypropylene (Usuki *et al.*, 1997; Kawasumi *et al.*, 1997; Hasegawa *et al.*, 1998; Marchant *et al.*, 2002). The dispersion of silicate layers strongly depends on the preparation techniques, such as in-situ polymerization, solution blending, or melt compounding. In this work, PP/clay nanocomposites are obtained by direct melt compounding of PP with organic MMT in the presence of maleic anhydride-grafted PP (PP-*g*-MA). This method was firstly developed by researchers at Toyota Central R & D Laboratories (Kawasumi *et al.*, 1997). They added three times as much PP-*g*-MA as the clay by weight in preparing well-mixed PP/clay nanocomposites. Thereafter the melt compounding intercalation method is being recognized as a promising approach because of its ease of employing conventional compounding process, although the successful result of in-situ polymerization method was reported recently (Sun *et al.*, 2002). For non-polar polymers such as PP, unless the organoclay is further treated with compatibilizers, applying high shear alone during melt compounding does not cause the clay tactoid to be delaminated. Efforts were made to improve the mixing of clay in PP by using functional oligomers as compatibilizers.

The objective of this study is to investigate the effect of compatibilizer type and compounding condition on the clay dispersion and mechanical properties of PP/clay nanocomposites, such as stiffness, strength, and impact resistance.

2. EXPERIMENTAL

2.1. Materials

The matrix PP used for this study was block-PP which was produced by Polymirae Company, Korea. The grade name is EP641P. (Density = 0.905 g/cm^3, Melt Flow Rate = 20 g/ 10 min at 230°C, 2.16 kg load) Four types of maleic anhydride-grafted PP (PP-*g*-MA) containing different amounts of maleic anhydride group were used in this study, PH-200 (containing 2.6 wt % maleic anhydride, supplied by Honam Petrochemical Co., Mw = 49,600), Epolene-43 (containing 4.2 wt % maleic anhydride, supplied by Eastman Chemical Co., Mw = 18,700), Polybond-3002 (containing 0.2 wt % maleic anhydride, supplied by Crompton, Melt Flow Rate = 7 g/ 10 min at 230°C, 2.16 kg laod), and Polybond-3200 (containining 1.0 wt % maleic anhydride, supplied by Crompton, Melt Flow Rate = 110 g/10 min at 190°C, 2.16 kg load). The commercial organic modified montmorillonite, Cloisite 20A, supplied by Southern Clay Products was used, which was ion-exchanged with dimethyl dehydrogenated tallow ammonium ions. (Tallow was composed predominantly of dodecyl chains with smaller amount of lower homologues. The approximate composition was C18 65%, C16 30% and C14 5%.)

2.2. Compounding and Preparation of PP/Clay Nanocomposites

In this study, PP/clay nanocomposites were prepared by a two-step compounding process. Firstly, PP-*g*-MA powder

Table 1. Compounding formulations of the first compounded master batch composites and the second compounded products.

Formulation Code	Block-PP EP641P [wt %]	PH-200 [wt %]	Epolene-43 [wt %]	Polybond-3002 [wt %]	Polybond-3200 [wt %]	Organo Clay [wt %]
1st Compounding (PP-g-MA and clay compounding)						
MB-1	–	70	–	–	–	30
MB-2	–	–	70	–	–	30
MB-3	–	–	52.5	17.5	–	30
MB-4	–	–	35	35	–	30
MB-5	–	–	17.5	52.5	–	30
MB-6	–	–	–	–	70	30
MB-7	–	60	–	–	–	30
2nd Compounding (block-PP and MB compounding)						
P-1	67	23	–	–	–	10
P-2	67	–	23	–	–	10
P-3	67	–	17.3	5.7	–	10
P-4	67	–	11.5	11.5	–	10
P-5	67	–	5.7	17.3	–	10
P-6	67	–	–	–	23	10
P-7	75	13	–	–	–	10

or pellet and the organoclay were premixed in a tumbling mixer together with 0.2 wt % of stabilizer. The mixture was melt-blended in a co-rotating twin screw extruder (Werner & Pfleiderer; ZSK 25) at 150–190°C and 150 r.p.m. The screw consisted of 10 segmented barrels with three kneading zones. The major processing variables were screw speed, barrel temperature profiles, and throughput rate. After several trials, the screw speed was set at 150 r.p.m and the barrel temperatures were set from 150°C at the first barrel to 190°C at the last barrel for the first compounding step. The obtained strands were pelletized and then dried at 80°C for 4 h. The compositions of the samples are summarized in Table 1. These first step compounding samples are master batches containing 30–40 wt % organoclay. (The sample names are abbreviated as MB-1, 2, 3, 4, 5, 6, 7) Secondly, the dried master batch composite pellets obtained in the previous step were premixed with neat block-PP pellets in a tumbling mixer together with 0.2 wt % of stabilizer. The mixtures were melt-blended in a co-rotating twin screw extruder (Werner & Pfleiderer; ZSK 25) at 190–230°C and 300 r.p.m. In the second compounding step, the screw speed was set at 300 r.p.m and the throughput rate was 2.0 kg/h. The obtained strands were pelletized and then dried at 80°C for 4 h. The compositions of the samples are also summarized in Table 1. The dried pellets were injection-molded into ASTM specimens for mechanical testing. The temperature of the cylinder was 200–235°C and that of the mold was at 40°C.

2.3. Characterization

X-ray diffraction (XRD) analysis was carried out by using Nanostar, Bruker X-ray diffractometer (Cu Ka radiation with $\lambda = 0.15406$ nm, generator voltage = 30 kV, current = 45 mA) at room temperature. The diffractogram were scanned in 2θ ranges from 1.0 to 10° at a rate of 1°/min. Measurement were recorded at every 0.03°. For comparative purpose, the XRD patterns were represented in terms of relative intensities; the intensity of the strongest reflection was arbitrarily assigned a value of d_{001}, the interplanar distance.

Bright field transmission electron microscopy (TEM) images of nanocomposites were obtained at an acceleration voltage of 120 kV operating power with a JEOL JEM-2000 EXII TEM. The nanocomposite samples, embedded in an epoxy resin and cured at 80°C overnight, were microtomed to give sections with a thickness of 70 nm. Ultra thin sections were prepared with a 45° diamond knife at room temperature using a Leica Ultracut UCT microtome. The sections were transferred from water to carbon-coated Cu grids of 200 mesh. The contrast between the layered silicates and the polymer was sufficient for imaging, so no heavy metal staining of sections prior to imaging, was required.

The tensile and flexural properties were measured with an Instron 4202 universal testing machine and the notched impact strength was measured with an impact tester Zwick, model 5102. The data were obtained at 23°C. All measurements were performed in five replicates and the values were averaged.

3. RESULTS AND DISCUSSION

Figure 1(a) shows the XRD patterns of first compounded master batch composites where peaks correspond to the (001) plane reflections of the clays. Four types of PP-*g*-MA containing different amounts of maleic anhydride group were used. In case of PH-200 containing 2.6 wt % maleic anhydride group (MB-1), there are no peaks in the XRD pattern. In case of Epolene-43 containing 4.2 wt % maleic anhydride group (MB-2), it was impossible to take strands continuously during the compounding operation in twin screw extruder. This was because the molar mass of Epolene-43 was very low and consequently the melt viscosity of that was also very low at the compounding operation temperature. The XRD pattern for MB-2, not shown here, displayed prominent clay peaks. The ineffective compatibilizer in this study, Epolene-43, has a

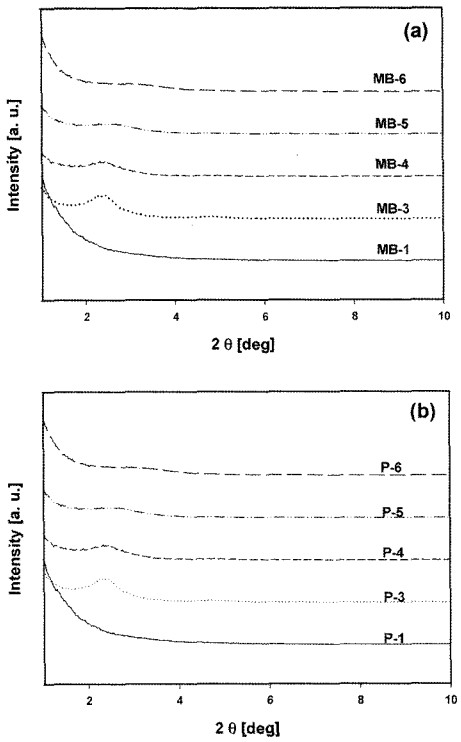

Figure 1. X-ray diffraction patterns of: (a) 1st compounded PP-*g*-MA/clay nanocomposites; (b) 2nd compounded block-PP/master batches (PP-*g*-MA/clay nanocomposites) nanocomposites.

weight average molecular weight of 18,700. Fornes *et al.* (2001) have reported a molecular weight dependence on the effectiveness of a compatibilizer. They investigated the exfoliation of clay in polyamide/clay nanocomposites. Their work used three different weight average molecular weight matrix resin; a low molecular weight, 16,400, a medium molecular weight, 22,000, and a high molecular weight, 29,300, polyamide. They found that the polyamide/clay composite formed with the low weight average molecular weight, 16,400, polyamide exhibited the least exfoliated clay structure. Their explanation of this observation is that the low molecular weight matrix resin is less efficient in transferring the stress from the shear field to the clay during processing. Therefore, in order to effectively transfer stresses from the polymer melt to the clay, the polymer chains must entangle. Epolene-43 didn't have a high degree of entanglements and thus was a poor agent to transfer stresses from the polymer melt to the clay in order to exfoliate the clay layers. To vary the maleic anhydride content in the compatibilizer, we tried to use the mixtures of Epolene-43 and Polybond-3002 having a sufficiently high molecular weight and 0.2 wt % maleic anhydride group. The contents of maleic anhydride group in these mixtures are 2.2 wt % (MB-3), 1.5 wt % (MB-4), and 0.2 wt % (MB-5) respectively. The XRD patterns of composites, MB-3, 4, 5 exhibit the clay peak or shoulders. In case of Polybond-3200 containing 1.0 wt % maleic anhydride group (MB-6), there is also small clay peak shoulder but the intensity is lower relatively. From the comparison of XRD patterns of MB-1 and MB-6, it is obvious that maleic anhydride group improves the dispersibility of the clays in the composites. But in cases of MB-5, 4, 3, as the content of maleic anhydride group increases, the intensity of clay peak in XRD patterns also increases. This result suggests that only Polybond-3002 was effective on the clay exfoliation in the mixture of Polybond 3002 and Epolene-43 during compounding operation. As mentioned above, the molar mass of Epolene-43 is low and therefore the melt viscosity of Epolene-43 is low under this compounding condition. No shear force could exert between the clay and Epolene-43. Figure 1(b) shows the XRD patterns of second compounded neat block-PP/MBs composites. In comparison with Figure 1(a), XRD patterns in Figure 1(b) are very similar to those in Figure 1(a). From these results, it is inferred that once the clay dispersion morphology have been formed in the first compounding step, the dilution of neat PP and the additional shear force exerted in the second compounding step doesn't affect the clay dispersion.

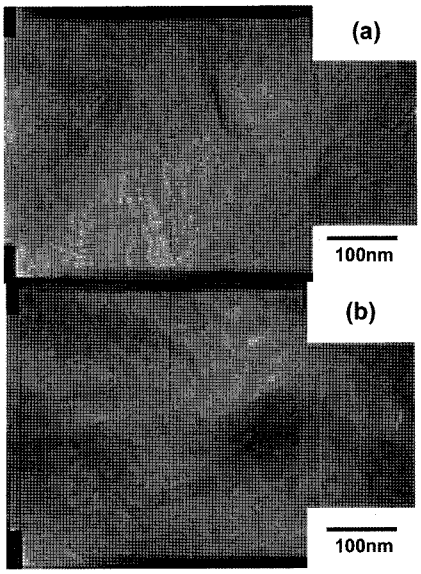

Figure 2. TEM images of P-1 and P-7 nanocomposites, containing 10 wt % clay: (a) P-1; (b) P-7.

Figure 2 shows TEM images of formulation code, P-1 and P-7 which were prepared by a two-step compounding process. As a compatibilizer, PH-200 is used for these two composites. The ratio of PP-*g*-MA to the clay is 2.3 in P-1 and 1.5 in P-7. Figure 2(a) shows that the particles of silicate layers are dispersed at the nanometer level. Each layer of the clay is dispersed homogeneously in the PP matrix. On the other hand, there are some aggregates of the clay layers at the micrometer level in Figure 2(b). This is because the ratio of PP-*g*-MA to clay in Figure 2(a) is higher than that in Figure 2(b).

Table 2 summarizes the mechanical properties of PP nanocomposites prepared by a two-step compounding process and neat block-PP/talc microcomposite which contains 7 wt % talc. Both the tensile strength and flexural modulus increase with increasing the ratio of PP-*g*-MA to clay in nanocomposites P-1 and P-7. It is noteworthy that the tensile strength and flexural modulus

Table 2. Mechanical properties of PP/clay nanocomposites prepared by 2-step compounding process.

Sample Code	Tensile Strength [kgf/cm^2]	Elongation [%]	Flexural Modulus [kgf/cm^2]	Impact Strength [kgf-cm/cm]	Shrinkage [^{o}/oo]
P-1	333	10	22800	4.2	7.0
P-7	291	12	20700	4.1	9.8
PP/talc	255	44	17060	9.5	13

Table 3. Compounding formulations of waist line molding and cowl top cover prepared by using PP/clay nanocomposite and their mechanical properties.

Properties	Waist line molding		Cowl top cover	
	Conventional PP composites	New nano-composite	Conventional PP composites	New nano-composite
Formulation [wt %]	PP : 40~60 Rubber : 10~15 Talc : 30~ 35	MB-7 : 35 Rubber : 20 PP : 45	PP : 60 Talc : 40	MB-7 : 50 Rubber : 5 PP : 45
Inorganic content [wt %]	30~35	9.2	40	13.2
Melt index [g/10 min]	8	2.4	7	0.2
Density [g/cm^3]	1.12	0.975	1.25	1.01
Tensile strength [kgf/cm^2]	200	273	270	304
Elongation [%]	20	15	10	8
Flexural modulus [kgf/cm^2]	14000	22570	35000	33150
Impact strength [kgf-cm/cm]	6.5	5.6	4	3.2
Shrinkage [°/oo]	5.0	4.0	8.0	5.6

of P-1 are about 1.3 times higher than that of neat PP/talc composite. The role of the clay as a reinforcement in the nanocomposite is evident. But the impact strength of clay nanocomposites is much lower than that of neat PP/talc composite. This is due to the unavoidable addition of lower molar mass of PP-*g*-MA compatibilizer for the clay exfoliation. In other words, a large portion of low molar mass compatibilizer forms a matrix phase together with neat PP. During the process of free radical maleic anhydride grafting onto PP backbone chain, PP chain scission is accompanied, consequently the lower molar mass of corresponding PP-*g*-MA is produced. High content of such oligomer in composite can adversely affect impact performance. Moreover, incompatibility problems between matrix PP and PP-*g*-MA could arise at high maleic anhydride content of PP-*g*-MA. So lower compatibilizer content, or higher compatibilizer molar mass, would be required to improve the toughness/stiffness balance of such compounds. We made two automotive parts, i.e. waist line molding and cowl top cover by using PP/clay nanocomposties. Table 3 shows the formulation and mechanical properties of conventional PP composites and new nanocomposites. Figure 3 and 4 show the images of injection-molded waist line molding and cowl top cover. As mentioned above, compared with conventional talc added composites, clay nanocomposites show the improvements in tensile strength and flexural modulus as well as low shrinkage, one of the key factors in dimensional stability and an essential factor to manufacture large vehicle parts by using smaller inorganic particles. These improvements, however, are offset by decreases in toughness.

Figure 3. Image of injection-molded waist line molding prepared by using PP/clay nanocomposite.

Figure 4. Image of injection-molded cowl top cover prepared by using PP/clay nanocomposite.

4. CONCLUSIONS

In this work, PP/PP-*g*-MA/clay nanocomposites were prepared by a two-step melt compounding process. As the ratio of PP-*g*-MA to clay increased, the dispersibility of clays increased. It seemed that the clay dispersion morphology was determined in the first compounding step and the dilution of neat PP and additional shear force exerted in the second compounding step didn't have influence on the clay exfoliation. For the effective continuous operation of twin-screw extruder compounding processing, it was necessary to use PP-*g*-MA having medium molecular weight and moderate degree of grafting. Strength and stiffness increased with the extent of clay exfoliation, but impact resistance decreased. This reduction in toughness was attributed to the addition of lower molar mass PP-*g*-MA to exfoliate clay layers. Ongoing research is aimed at the effect of high molar mass PP-*g*-MA on impact property and clay exfoliation.

ACKNOWLEDGEMENT–We acknowledge the financial support from Hyundai Motor Company, South Korea.

REFERENCES

Fornes, T. D. Yoon, P. Keskkula, J. H. and Paul, D. R. (2001). Nylon 6 nanocomposites: the effect of matrix molecular weight. *Polymer*, **42**, 9929–9940.

Frohlich, J. Thomann, R. and Mulhaupt, R. (2003). Toughened epoxy hybrid nanocomposites containing both an organophilic layered silicate filler and a compatibilized liquid rubber. *Macromolecules*, **36**, 7205–7211.

Hasegawa, N. Kawasumi, M. Kato, M. Usuki, A. and Okada, A. (1998). Preparation and mechanical properties of polypropylene-clay hybrids using a maleic anhydride-modified polypropylene oligomer. *J. Appl. Polym. Sci.*, **67**, 87–92.

Im, K. H. Park, N. S. Kim, Y. N. and Yang, I. Y. (2003). A study om impact characteristics of the stacking sequences in cfrp composites subjected to falling weight impact loading. *Int. J. Automotive Technology* **4**, **4**, 203–211.

Kawasumi, M. Hasegawa, N. Kato, M. Usuki, A. and Okada, A. (1997). Preparation and mechanical properties of polypropylene-clay hybrids. *Macromolecules*, **30**, 6333–6338.

Kim, J. W. Liu, F. H. and Choi, J. (2002). Polypyrrole/clay nanocomposite and its electrorheological characteristics. *J. Ind. Eng. Chem.*, **8**, 399–403.

Li, X. C. Kang, T. Cho, W. J. Lee, J. K. and Ha, C. S. (2001). Preparation and characterization of poly(butyleneterephthalate)/organoclay nanocomposites. *Macromol. Rapid Commun.*, **22**, 1306–1312.

Lim, S. T. Choi, H. J. and Jhon, M. S. (2003). Dispersion quality and rheological property of polymer/clay nanocomposites: ultrasonification effect. *J. Ind. Eng. Chem.*, **9**, 51–57.

Marchant, D. and Jayaraman, K. (2002). Strategies for optimizing polypropylene-clay nanocomposite structure. *Ind. Eng. Chem. Res.*, **41**, 6402–6408.

Sun, T. and Garces, J. M. (2002). High-performance polypropylene-clay nanocomposites by In-situ polymerization with metallocene/clay catalysts. *Adv. Mater.*, **14**, 128–130.

Tyan, H. L. Liu, Y. C. and Wei, K. H. (1999). Enhancement of imidization of poly(amic acid) through forming poly(amic acid)/organoclay nanocomposites. *Polymer*, **40**, 4877–4886.

Usuki, A. Kato, M. Okada, A. and Kurauchi, T. (1997). Synthesis of polypropylene-clay hybrid. *J. Appl. Polym. Sci.*, **63**, 137–138.

Vaia, R. A. Jandt, K. D. Kramer, E. J. and Giannelis, E. P. (1996). Microstructural evolution of melt intercalated polymer-organically modified layered silicates nanocomposites. *Chem. Mater.*, **8**, 2628–2635.

Wu, Z. G., Zhou, C. X. Qi, R. R. and Zhang, H. B. (2002). Synthesis and characterization of nylon 1012/clay nanocomposite. *J. Appl. Polym. Sci.*, **83**, 2403–2410.